Ecotoxicology and Environmental Safety 208 (2021) 111437

Contents lists available at ScienceDirect

Ecotoxicology and Environmental Safety

journal homepage: www.elsevier.com/locate/ecoenv

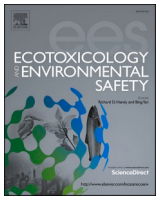

Fluoride exposure during pregnancy and lactation triggers oxidative stress and molecular changes in hippocampus of offspring rats

Maria Karolina Martins Ferreira [a], Walessa Alana Bragança Aragão [a], Leonardo Oliveira Bittencourt [a], Bruna Puty [a], Aline Dionizio [b], Michel Platini Caldas de Souza [c], Marilia Afonso Rabelo Buzalaf [b], Edivaldo Herculano de Oliveira [c], Maria Elena Crespo-Lopez [d], Rafael Rodrigues Lima [a,*]

[a] Laboratory of Functional and Structural Biology, Institute of Biological Sciences, Federal University of Pará, Belém, Brazil
[b] Department of Biological Sciences, Bauru Dental School, University of São Paulo, Bauru, São Paulo, Brazil
[c] Laboratory of Cell Culture and Cytogenetics, Environment Section, Evandro Chagas Institute, Ananindeua, Brazil
[d] Laboratory of Molecular Pharmacology, Institute of Biological Sciences, Federal University of Pará, Belém, Brazil

ARTICLE INFO

Edited by Dr. Fernando Barbosa

Keywords:
Fluoride
Offspring
Neurotoxicity
Oxidative stress
BDNF
Proteomic

ABSTRACT

Long-term exposure to high concentrations of fluoride (F) can damage mineralized and soft tissues such as bones, liver, kidney, intestine, and nervous system of adult rats. The high permeability of the blood–brain barrier and placenta to F during pregnancy and lactation may be critical to neurological development. Therefore, this study aimed to investigate the effects of F exposure during pregnancy and lactation on molecular processes and oxidative biochemistry of offspring rats' hippocampus. Pregnant Wistar rats were randomly assigned into 3 groups in accordance with the drinking water received: G1 – deionized water (control); G2 – 10 mg/L of F and G3 – 50 mg/L of F. The exposure to fluoridated water began on the first day of pregnancy and lasted until the 21st day of breastfeeding (when the offspring rats were weaned). Blood plasma samples of the offspring rats were collected to determine F levels. Hippocampi samples were collected for oxidative biochemistry analyses through antioxidant capacity against peroxyl (ACAP), lipid peroxidation (LPO), and nitrite (NO_2^-) levels. Also, brain-derived neurotrophic factor (BDNF) gene expression (RT-qPCR) and proteomic profile analyses were performed. The results showed that exposure to both F concentrations during pregnancy and lactation increased the F bioavailability, triggered redox imbalance featured by a decrease of ACAP, increase of LPO and NO_2^- levels, BDNF overexpression and changes in the hippocampus proteome. These findings raise novel questions regarding potential repercussions on the hippocampus structure and functioning in the different cognitive domains.

1. Introduction

Humans can be exposed to fluoride (F) through water, air, fish, vitamin supplements, agrochemicals (organofluorides), and some dental products (Buzalaf et al., 2011; Dhar and Bhatnagar, 2009; Hagmann, 2008; Varner et al., 1998). Although this semi-essential mineral element plays a key role in preventing tooth caries, the excessive exposure to F has been associated with adverse reactions such as fluorosis (Miranda et al., 2018; Shenoy et al., 2019), which is considered an endemic public health problem in several nations and can also affect bones and soft tissues such as the brain, liver, kidney, gonads, and spinal cord (Ozsvath and Bio/Technology, 2009).

Epidemiological studies in some areas with endemic fluorosis have found an inverse relationship between children's intelligence quotient and F levels (Karimzade et al., 2014; Trivedi et al., 2012). Similarly, a meta-analysis has indicated a strong association between dental fluorosis and low IQ in Chinese children (Tang et al., 2008), while other studies carried out in India also showed IQ deficits in children with dental fluorosis (Saxena et al., 2012; Shivaprakash et al., 2011). However, there are no evidences that artificial fluoridation of water in ideal concentration may cause any other systemic effects (Cury et al., 2019).

Recent animal studies have evidenced that F can cross the

* Corresponding author: Laboratory of Functional and Structural Biology, Institute of Biological Sciences, Federal University of Pará, 01 Augusto Corrêa Street, Guamá, 66075-110 Belém, PA, Brazil.
E-mail address: rafalima@ufpa.br (R.R. Lima).

https://doi.org/10.1016/j.ecoenv.2020.111437
Received 10 June 2020; Received in revised form 24 September 2020; Accepted 28 September 2020
Available online 20 October 2020
0147-6513/© 2020 Elsevier Inc. This is an open access article under the CC BY-NC-ND license (http://creativecommons.org/licenses/by-nc-nd/4.0/).

blood–brain barrier and modify neural circuits of several areas such as the cerebellum, motor cortex, and hippocampus (Dec et al., 2017, 2019), triggering functional deficits in learning and memory and anxiety-depression behaviors (Jiang et al., 2014a; Li et al., 2019; Liu et al., 2014; Zhu et al., 2017). The hippocampus integrates the projections of other structures, such as the entorhinal, perirhinal, and para-hippocampal cortices (Squire, 1992) and plays important roles in the formation of spatial, visual, and recognition memories (Barker and Warburton, 2015; Broadbent et al., 2004; Clark et al., 2000). Moreover, it is one of the central nervous system (CNS) structures most affected by F intoxication (Zhang et al., 1999). In addition, previous studies have pointed that fluorosis can modify the synaptic structure of the hippocampus (Niu et al., 2018; Qian et al., 2013) and may influence the transmission of neural information (Shivarajashankara et al., 2002).

Alterations in the CNS are more accentuated up to 6th month of pregnancy due to the incomplete development of blood–brain barrier that allows the passage of F and consequent damage to the brain structures (Kinawy and Research, 2019). In comparison to the mature brain, F exposure increases the vulnerability of the developing nervous system to permanent injuries caused by toxic substances due to the immature defense mechanisms (Grandjean and Landrigan, 2006).

In this way, from a translational perspective, the exposure to F in this development period has been pointed as capable of triggering neurobehavioral changes in children such as attention deficit hyperactivity disorder (Bashash et al., 2018). However, there are no evidences that premature exposure to F during pregnancy and lactation causes molecular damages.

Therefore, this study aimed to investigate the effects of the exposure to F during pregnancy and lactation of rats on molecular, biochemical, and proteomic parameters. The null hypothesis tested was that F exposure during these periods does not have a significant influence on the oxidative biochemistry, proteomic profile modulation, and cellular function of offspring rats' hippocampus.

2. Material and methods

2.1. Animals and treatment

The experimental protocol (register 2718220318) was approved by the Ethics Committee for Animal Experiments of Federal University of Pará, Brazil, according to NIH Guide for the Care and Use of Laboratory Animals recommendations.

A total of six female Wistar rats (150 ± 200 g) with 90-day old and pregnant, were randomly divided into three groups: control (0 mg/L), 10 mg/L and 50 mg/L of F. The concentrations 10 mg /L and 50 mg /L of F are equivalent to the consumption of artificially fluoridated water and in fluorosis endemic regions, respectively, adapted to the rodent metabolism (Dunipace et al., 1995; Whitford, 2011). The confirmation of pregnancy was determined by vaginal tampon identification (G0). The animals were maintained with ad libitum access to food and water, controlled temperature and humidity, and with regular light/dark cycles (12 h, lights on at 6 a.m.). The control group received deionized water and the exposed groups received solution of deionized water with the corresponding concentrations of F (as NaF, Sigma Chemical - EUA), during 42 days (21 days of pregnancy and 21 days of lactation). After lactation period, the blood and hippocampus samples were collected from the offspring (21-day old). The study design is shown in Fig. 1.

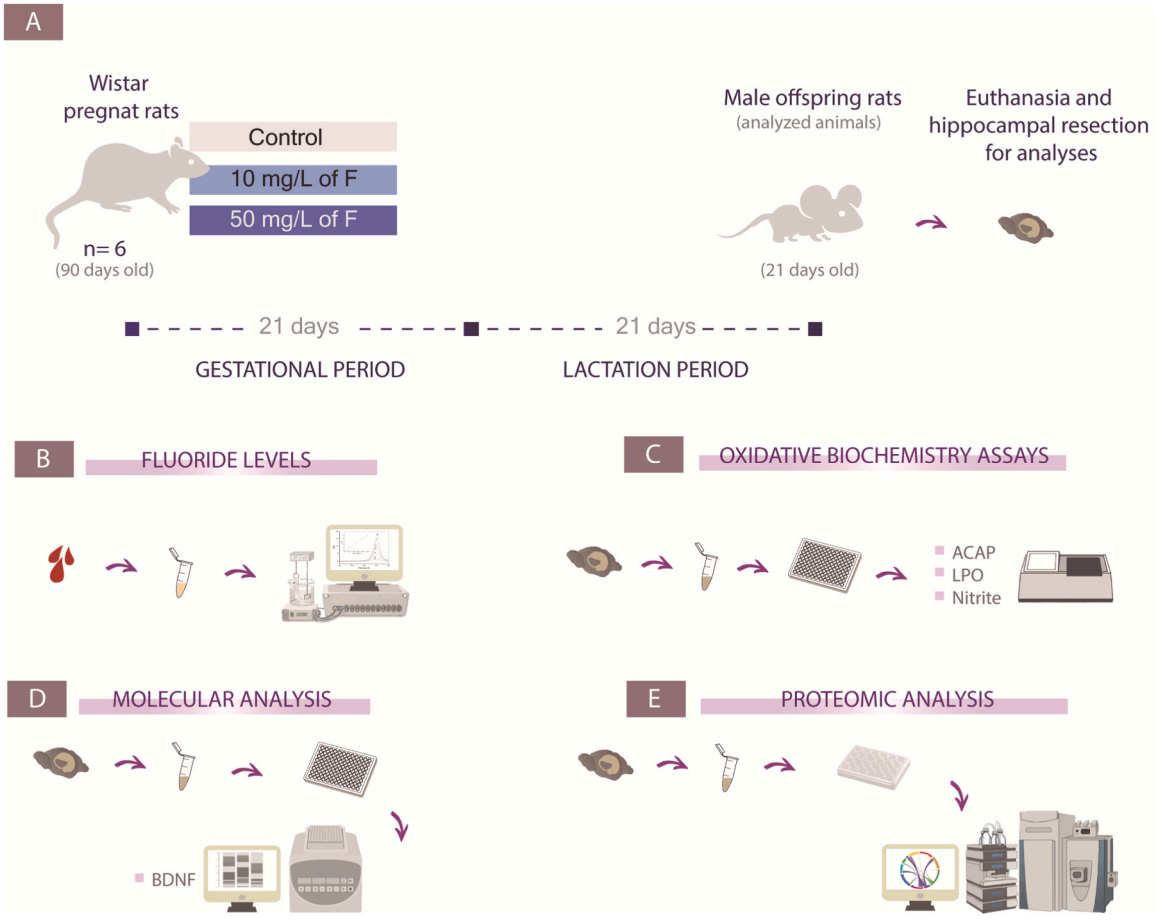

Fig. 1. Study design. (A) Exposure protocol followed by samples collection for: (B) Determination of plasma fluoride levels; (C) Oxidative biochemistry; (D) Molecular analysis; and (E) proteomic analysis.

2.2. Sample preparation

The blood samples were collected in heparinized tubes and centrifuged at 696 g for 10 min and then, the plasma of each sample was stored in microtubes until F analysis. The hippocampi were collected, stored in microtubes and immediately frozen in liquid nitrogen, and later stored at − 80 °C for further analyses.

2.3. Fluoride concentration in plasma

This analysis was proceeded as described elsewhere (Taves, 1968; Whitford, 2011) and was performed in order to validate our exposure model. For this analysis, we used a specific ion F electrode (Orion Research, Model 9409) and a miniature calomel electrode (Accumet #13-620-79), both coupled to a potentiometer (Orion Research, Modelo EA 940). The plasma was prediffused to remove CO_2. The F concentrations in plasma were determined after acid-hexamethyldisiloxane (HMDS)-facilitated microdiffusion. F standards (0.0048 - 0.19 μg F) were prepared in triplicate and diffused similarly as the samples. Non-diffused standards were prepared with the same concentrations as the diffused standards. The millivoltage (mV) readings were converted into μg F using Excel (Microsoft). The coefficient adopted to standard curve was $r \geq 0.99$. The comparison of the mV readings showed a complete extraction of fluoride (recovery higher than 95%). The F concentration was expressed in μg/mL.

2.4. Hippocampal oxidative biochemistry analyses

Initially, each sample was sonically homogenized with Tris-HCl buffer (pH 7.4, 29 mM) and divided into different aliquots (correspondent to each assay described below) and stored at − 80 °C. The homogenized samples were centrifuged at 21.000 g for antioxidant capacity against peroxyl radicals and nitrite analyses and at 2.500 g for lipid peroxidation and total protein content determination assays, using only the supernatant for each analysis.

2.4.1. Antioxidant capacity against peroxyl radicals (ACAP)

This analysis was performed according to the protocol described elsewhere (Amado et al., 2009). After defrosting the samples, 10 μL of supernatant from each sample were placed in six wells in a 96-well plate. The reaction buffer (127.5 μL) containing 30 mM HEPES (pH 7.2), 200 mM KCl and 1 mM $MgCl_2$ were added to the wells. In three of the six wells of each sample, 7.5 μL of 2,2′-azobis 2 methylpropionamidine dihydrochloride (ABAP; 4 mM; Aldrich) were added to produce peroxyl radicals by thermal decomposition. In the other three wells, the same volume of water was pipetted. Subsequently, the microplate was placed in a microplate reader fluorimeter (Victor2, Perkin Elmer) at 35 °C. After the first reading, 10 μL of 2′,7′ dichlorofluorescein diacetate (H 2 DCF-DA) in a concentration of 40 nM were added and then monitored for 60 min with consecutive readings every 5 min. The relative difference between the area with ABAP and the area without ABAP was considered as a measure of ACAP, so when the difference is high, it means low ACAP, since high fluorescence levels were obtained after the addition of ABAP, which means low competence to neutralize peroxyl radicals. The results were expressed as inverse of the relative area and then converted into percentage of control.

2.4.2. Levels of lipid peroxidation (LPO)

The LPO levels were determined by measuring the malonaldehyde (MDA) levels according to Esterbauer and Cheeseman (1990). In a 96-wells microplate, 20 μL of supernatant from each sample or standard concentrations of MDA were incubated with a solution containing methanesulfonic acid and *N*-methyl-phenyl indole (10.3 mM in acetonitrile) diluted in methanol (1:3) for 40 min at 45 °C. The absorbance was measured at 570 nm and compared to standard curve of MDA. The data were corrected by quantification of total proteins based on Bradford's method (Bradford, 1976) and then expressed in nmol/μg of protein and then converted into percentage of control.

2.4.3. Analysis of nitrite levels

This assay was carried out according to the study by Green et al., (1982). The concentration of nitrites was determined based on the reaction with the Griess reagent (Nafty-ethylene-diamine 0.1% and Sulfanilamide 1% in phosphoric acid 5% − 1:1). For this, 50 μL of the supernatant or standard nitrite solutions were added to 50 μL of the Griess reagent and incubated for 20 min in room temperature. The absorbances were read at 550 nm, the results were corrected by Bradford's method (Bradford, 1976), expressed in μmol/μg of protein and then converted into percentage of control.

2.5. RT-qPCR expression analysis

2.5.1. mRNA purification

After collection, the right hemisphere of each hippocampus was immersed in a microtube containing stabilizing reagent (RNAlater®) for later quantitative RT-qPCR technique in real-time. The extraction of the total mRNA from the samples was performed by SV total RNA isolation system kit (Promega®) according to the manufacturer's recommendations. The total RNA extracted was quantified by a Nanodrop spectrophotometer (ND-1000). The quality standards were determined by the ratio of 260/280 nm readings and the integrity parameters were performed according to the TapeStation software, in which the RIN values of each sample were considered.

Gene expression after fluoride exposure was validated using real-time quantitative RT-qPCR analysis. mRNA of each sample was used for reverse transcription through GoScript Reverse Trancription System kit (Promega®). Briefly, 100 ng of mRNA were add in 0.5 μg/reaction of Random Primer and incubated in 70 °C for 5 min. Then, 15 μL of reverse transcription master mix (GoScript buffer, MgCl2, dNTP, ribonuclease inhibitor and reverse transcriptase) were added in a solution with mRNA and primer and incubated according to the following set up 5 min at 25 °C for annealing, 1 h at 42 °C for extension and 15 min at 70 °C for reverse transcriptase inactivation. RT-qPCR analysis was performed with GoTaq probe qPCR Master Mix kit (Promega®). One microliter of each cDNA sample was added in 19 μL qPCR Master Mix plus with 1 μL of the Taqman probe (ThermoFisher, USA) Brain-derived neurotrophic factor (*BDNF; Rn02531967_s1; Forward TCATACTTCGGTTGCATGAAGG-Reverse AGACCTCTCGAACCTGCCC)* and Beta-actin *(ACTB; Rn00667869_m1; Forward ATCTGGCACCACACCTTC-Reverse AGCCAGGTCCAGACGCA*).

The analysis was carried out on the Bio-Rad CFX96 Real-Time PCR detection system. All reactions were performed in triplicate in 96-well PCR plate. Gene expression was normalized according to MIQE guideline (Bustin et al., 2009) and the relative gene expression was calculated according to the $2^{-\Delta\Delta Ct}$ formula (Livak and Schmittgen, 2001). Data were evaluated in the CFX Maestro program and considered when $p < 0.05$.

2.6. Proteomic analysis

2.6.1. Protein extraction

The proteomic analysis was performed according to the protocol previously described elsewhere (Bittencourt et al., 2019; Corrêa et al., 2020; Dionizio et al., 2018). For this, two samples from each group were pooled and analyses were carried out in triplicate. The samples were homogenized in a buffer solution for the extraction of soluble proteins with lysis buffer [7 M urea, 2 M thiourea, diluted in AMBIC; BioRad, USA] under constant stirring at 4 °C. Subsequently, the samples were centrifuged for 30 min at 20.817 g at 4 °C to collect the supernatant for total protein quantification by Bradford's method. In the next step, a total of 50 μg of protein were collected and the volume was filled with ammonium bicarbonate (AMBIC, 50 mM) up to 50 μL (1 μg μL^{-1}). After

that, each sample was incubated with 10 μL of 50 mM AMBIC and 25 μL of 0.2% RapiGEST™ (Waters Co., Manchester, UK) at 37 °C for 30 min. Then, 2.5 μL of 100 mM dithiothreitol were added and incubated at 37 °C for 60 min, immediately 2.5 μL of 300 mM iodoacetamide (Bio-Rad, USA) were added and incubated for 30 min at room temperature and in dark. To perform the protein digestion, 10 μL of trypsin (Thermo Fisher, USA) were added for 14 h at 37 °C, after that, 10 μL of 5% trifluoroacetic acid (Sigma-Aldrich, USA) were added and incubated for 90 min at 37 °C. At the end of the process, the samples were purified using C18 spin columns (Thermo Fisher, USA), concentrated until an approximate volume of 1 μL and resuspended in 12 μL of ADH (1pmol μL^{-1}) + 108 μL of 3% acetonitrile (Sigma-Aldrich, USA) and 0.1% formic acid (Thermo Fischer, USA).

2.6.2. Mass spectrometry analysis

The reading and identification of the peptides were performed using a nanoAcquity UPLCXevo QTof MS system (Waters, Manchester, UK), using the Protein Lynx Global Server (PLGS), as previously described by Lima Leite et al. (2014). For data analysis, we used the PLGS software with the Monte–Carlo algorithm to obtain the difference of protein expression between the groups, considering $p < 0.05$ for down-regulated proteins and 1-$p > 0.95$ for up-regulated proteins. The identification of proteins was determined by downloading Uniprot databases. After that, the bioinformatics analyses were performed using Cytoscapes 3.6 (Javas) with the ClueGO plugin for determination of biological process groups, based on Gene Ontology annotations (Bindea et al., 2009).

2.6.3. Overrepresentation analysis (ORA)

Firstly, a table was built containing the information with the accession ID of the proteins and their respective log2Ratio values. For proteins with absolute changes, a value of − 1 was adopted when present only in the control group and 1 when present in the exposed group. For the ORA analysis, the R studio program was used (Team, 2013) with EGSEA package (Alhamdoosh et al., 2017). In this step, the UNIPROT and Bader Lab database were consulted for the identification of proteins and their biological processes. Then, we used the Cytoscape software with Enrichment Pipeline plugin to create clusters of proteins previously consulted for graphic analysis (Shannon et al., 2003).

Subsequently, a protein–protein–interaction (PPI) analysis (https://www.networkanalyst.ca/) (Xia et al., 2014) was performed to construct the representative image, according to the number of interactions of the proteins with a minimum of 10 interactions, resulting in 81 proteins. The circus plot image was generated by the R studio program with the GOplot plugin.

2.7. Statistical analyses

The results were analyzed by GraphPad Prism 7.0 software (GraphPad Software Inc., La Jolla, USA) and for calculating the standard data distribution, the normality Shapiro–Wilk test was performed and the normal data were analyzed by one-way ANOVA followed by Tukey's test. The significance level adopted was $p < 0.05$.

Data were expressed as mean ± standard error of the mean (SEM) for each fluoride levels and percentage of the control mean ± SEM for oxidative biochemistry assays.

3. Results

3.1. The F Exposure during pregnancy and lactation periods increases F levels in the plasma of the offspring

The exposure increased F levels in the plasma of offspring in groups exposed to 10 mg/L (0.03 ± 0.002 μg/mL) and 50 mg/L (0.045 ± 0.005 μg/mL), when compared to control group (0.01 ± 0.009 μg/mL) ($p = 0.003$) (Fig. 2).

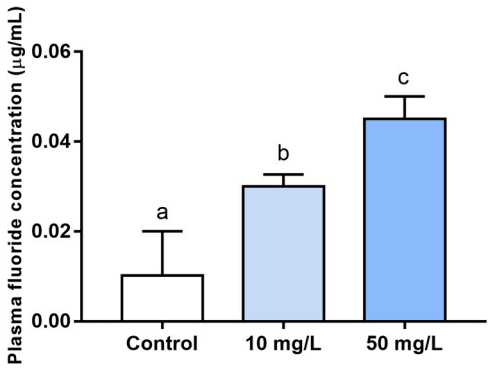

Fig. 2. Fluoride (F) levels (μg/mL) in the rats offspring' blood plasma after 42 days of exposure in pregnant and lactation period. Results are expressed as mean ± SEM. One-way ANOVA and Tukey's post hoc test, $p < 0.05$. Similar overwritten letters represent non-significant statistical differences.

3.2. The F exposure triggered oxidative stress by reducing the antioxidant capacity and increasing nitrite and LPO levels

The oxidative biochemistry analyses showed that the F caused a decrease of ACAP in 10 mg/L group (74.74 ± 7.46%) ($p = 0.01$) and in 50 mg/L group (46.88 ± 2.37%) when compared with control group [100 ± 6.63%, F (2, 15)] = 20.11, $p < 0.0001$)].

The oxidative parameters showed an increase in MDA levels, in both exposed groups, (10 mg/L (13.9 ± 1.54%) and in 50 mg/L (29.3 ± 1.53%) when compared to the control group [100 ± 0.038%, F (2, 20) = 120.7, $p < 0.0001$], and increase nitrite levels in 10 mg/L group (730.1 ± 23.31%) and 50 mg/L group (1041 ± 14.28%) in comparison to the control group [100 ± 14.13%, F (2, 19) = 611, $p < 0.0001$] (Fig. 3).

3.3. The F exposure increased BDNF expression in offsprings' hippocampus

Detailed mRNA analysis of whole hippocampus revealed that there was an increase BDNF expression in both groups exposed when compared with control group ($p < 0.05$) (Fig. 4).

3.4. . The F modulated significantly the hippocampal proteome of rats exposed from intrauterine to lactation periods

The hippocampal proteome analysis of rats exposed to 10 mg/L revealed 255 proteins uniquely expressed in control group (see supplementary table 1) and 16 uniquely in exposed group 10 mg/L (see supplementary table 2). While the proteome of 50 mg/L exposed group, showed 115 proteins that were only expressed in the control group (see supplementary table 3) and 55 only expressed in the exposed group 50 mg/L (see supplementary table 4).

Also, 10 mg/L down-regulated 108 proteins (see supplementary table 5) and no protein was up-regulated. In the other hand, 50 mg/L up-regulated 2 proteins and down-regulated 212 proteins, in comparison to control group (see supplementary table 6).

In group 10 mg/L of F that simulated consumption of artificially fluoridated water, were identified changes in proteins associated to axogenesis (23.4%), positive regulation of neuron projection development (19.1%), glycolytic process (9.9%) and regulation of calcium ion transport into cytosol (6.4%) (Fig. 5).

In the group of higher concentration, 50 mg/L of F, the most modified proteins were involved in morphogenesis of neuronal projection processes (18.1%), regulation of neuron projection development (15.1%), axogenesis (12%), glycolytic process (6.4%) and regulation positive of ERK 1 and 2 cascade (4.7%) (Fig. 6).

Based on the analysis of the proteomic profile, we compiled the data

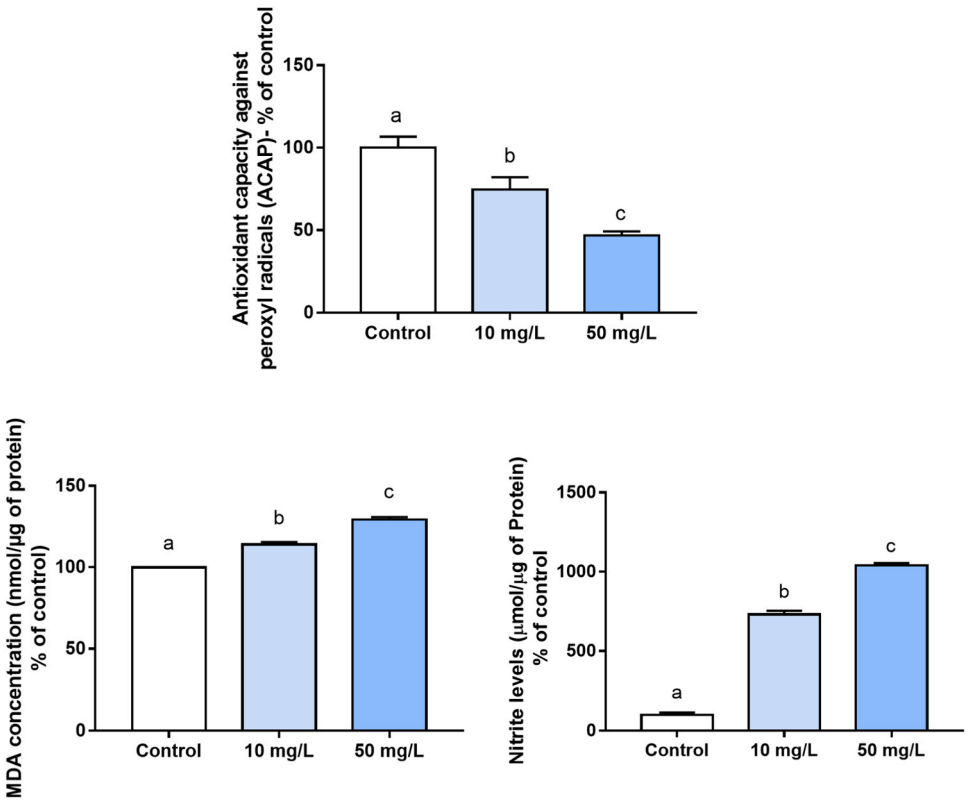

Fig. 3. Oxidative biochemistry profile in the rats offspring after 42 days of exposure to fluoride (F) in pregnant and lactation period. (A) Antioxidant capacity against peroxyl radicals (ACAP), (B) malondialdehyde (MDA) levels and (C) nitrite levels. Results are expressed as percentage of control (mean ± SEM). One-way ANOVA and Tukey's post hoc test, $p < 0.05$. Similar overwritten letters did not show significant statistical differences.

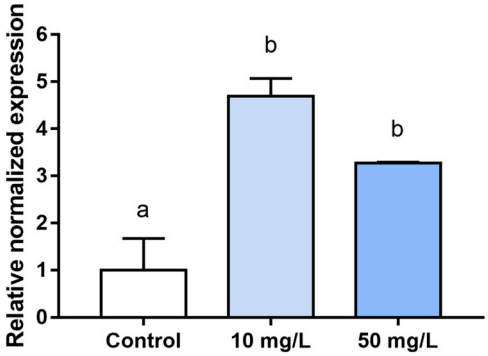

Fig. 4. Relative normalized expression in the BDNF after 42 days of exposure to fluoride (F) in pregnant and lactation period offspring's hippocampus. The BDNF was quantified in triplicate, according to the expression related to the constitutive gene β-actin. Results are expressed as mean ± SEM. One-way ANOVA and Tukey's post hoc test, $p < 0.05$. Similar overwritten letters did not show significant statistical differences.

to evaluate the protein–protein interaction, unique and with differing expression, of the exposed groups (10 mg/L vs 50 mg/L of F) and the functions that could be related, with the tool circos plot. Thus, it is possible to observe the interactions that each protein presented in each exposed group between proteins sub or super represented, as well as the absent proteins to each exposed group (Fig. 7).

4. Discussion

This study showed the unprecedented hippocampal proteomic profile of offspring rats exposed to F during their intrauterine life up to the end of lactation. The findings revealed several biological processes associated with glycolytic pathways, neuronal development, cellular signaling, and communication. Moreover, the increased bioavailability of F in plasma leads to an increase of BDNF expression and prooxidant parameters levels such as MDA and nitrites, which decreases the antioxidant capacity.

The changes caused by excessive F intake by adult rats have already been well established in the literature (Lima Leite et al., 2014; Miranda et al., 2018). It is known that F can cross the placental barrier and also is excreted in breast milk (Katz and Stookey, 1973; Toyama et al., 2001). Therefore, this study aimed to investigate the effects of F exposure during the intrauterine life and lactation of *Wistar* offspring rats. The data revealed higher F plasma levels in offspring rats exposed to fluoridated water in comparison to non-exposed offspring rats, which validates this study design. The concentrations of 10 mg/L and 50 mg/L were used to mimic F plasma levels observed in humans who drink fluoridated water (1–2 mg/L of F) and found in areas with endemic fluorosis (5–10 mg/L of F), which represents an excellent model to understand the effects caused by fluoride exposure (Dionizio et al., 2018; Dunipace et al., 1995; Miranda et al., 2018; Whitford, 2011).

Once ingested, F binds to hydrogen (H^+) present in the gastric fluid to form hydrofluoric acid that can cross cell membranes; thus, the F concentration in the tissues is pH-dependent (the lower the pH value, the higher the fluoride concentration). From plasma, F is distributed to all tissues, including the CNS since some epidemiological studies had already pointed the F as a neurotoxic substance (Buzalaf et al., 2011).

Several studies have shown that F levels may be associated with oxidative stress triggering. This research group recently showed that the same F concentrations modified the redox balance in the peripheral blood circulation of adult animals (Miranda et al., 2018). We believe that the oxidative balance of the CNS could be broken at an early age, featured by the decrease of antioxidant capacity and increase of MDA

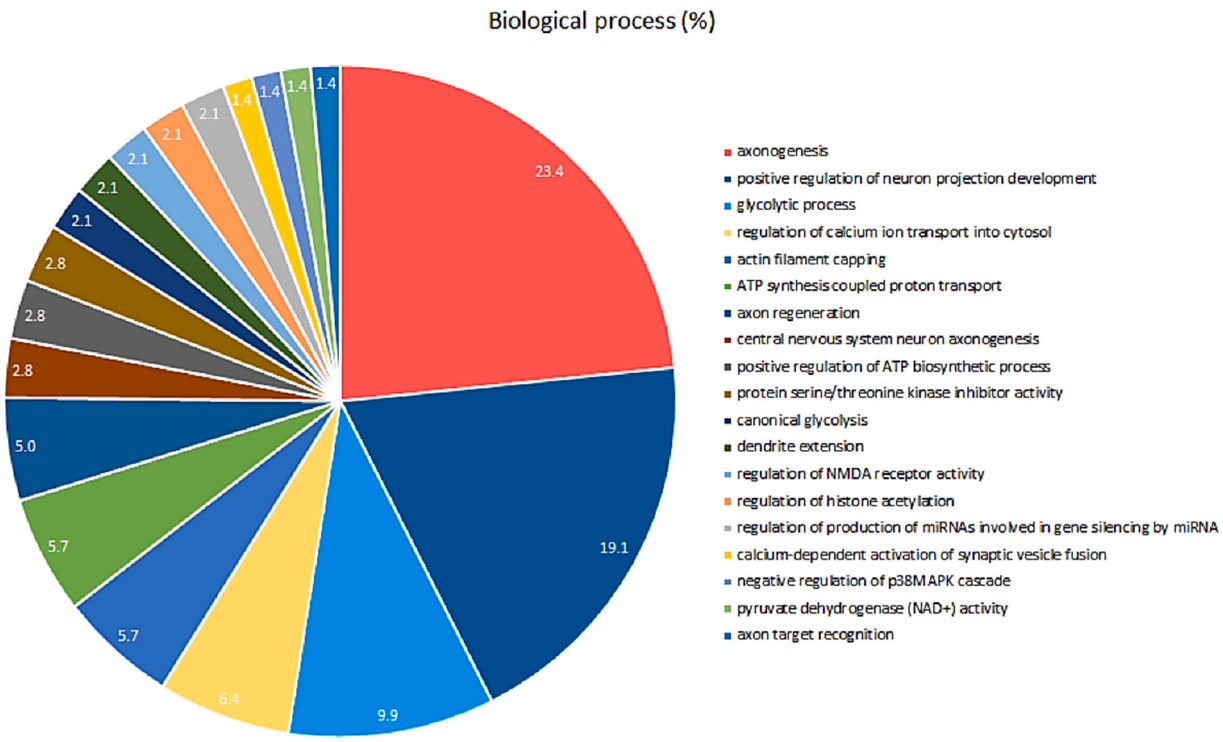

Fig. 5. Distribution of proteins identified with differential expression in the hippocampus of offspring exposed to fluoride (F) (10 mg/L of F) compared with control group. Proteins classified by biological processes based on Gene ontology, with the help of the ClueGo® plugin for Cytoscape® 3.6 software. Adopted the significant terms (kappa score = 0.4) and distribution according to the percentage of the number of genes. The access numbers to the proteins were obtained by UNIPROT.

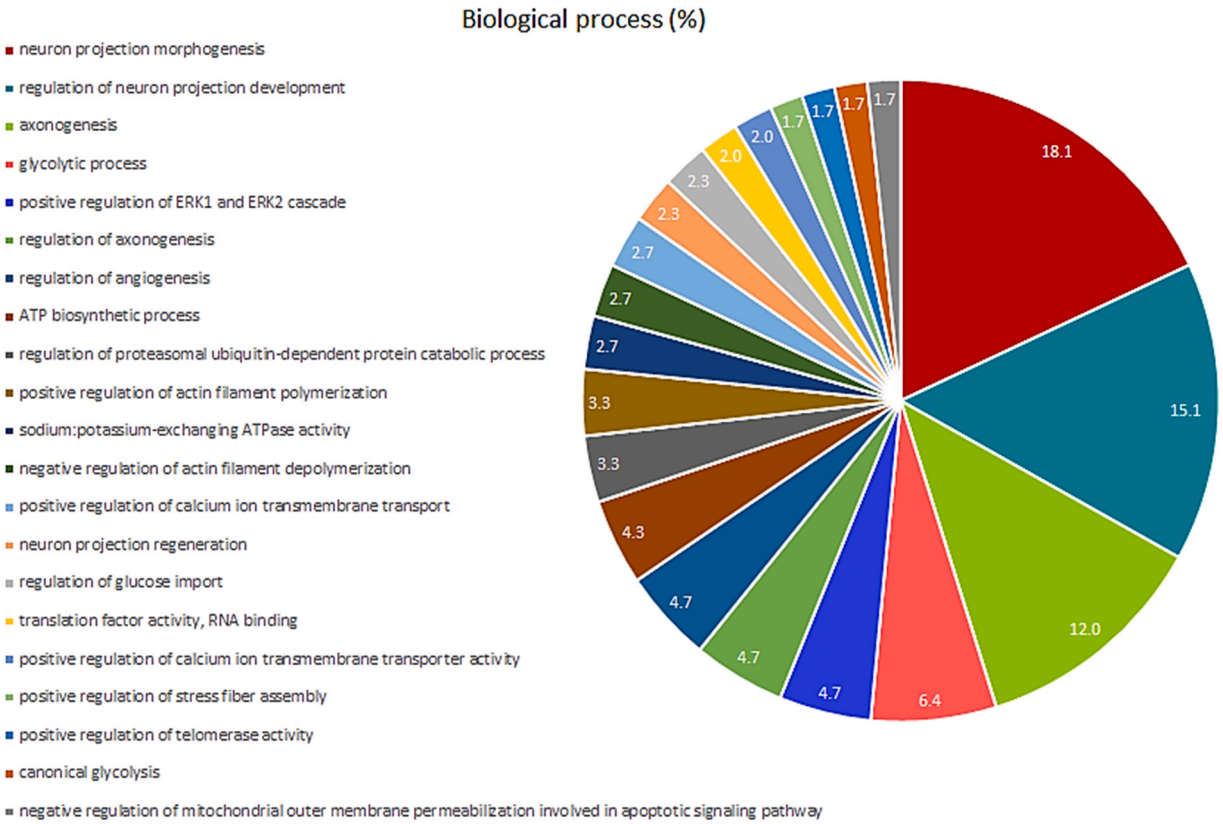

Fig. 6. Distribution of proteins identified with differential expression in the hippocampus of offspring exposed to fluoride (F) (50 mg/L of F) compared with control group. Proteins classified by biological processes based on Gene ontology, with the help of the ClueGo® plugin for Cytoscape® 3.6 software. Adopted the significant terms (kappa score = 0.4) and distribution according to the percentage of the number of genes. The access numbers to the proteins were obtained by UNIPROT.

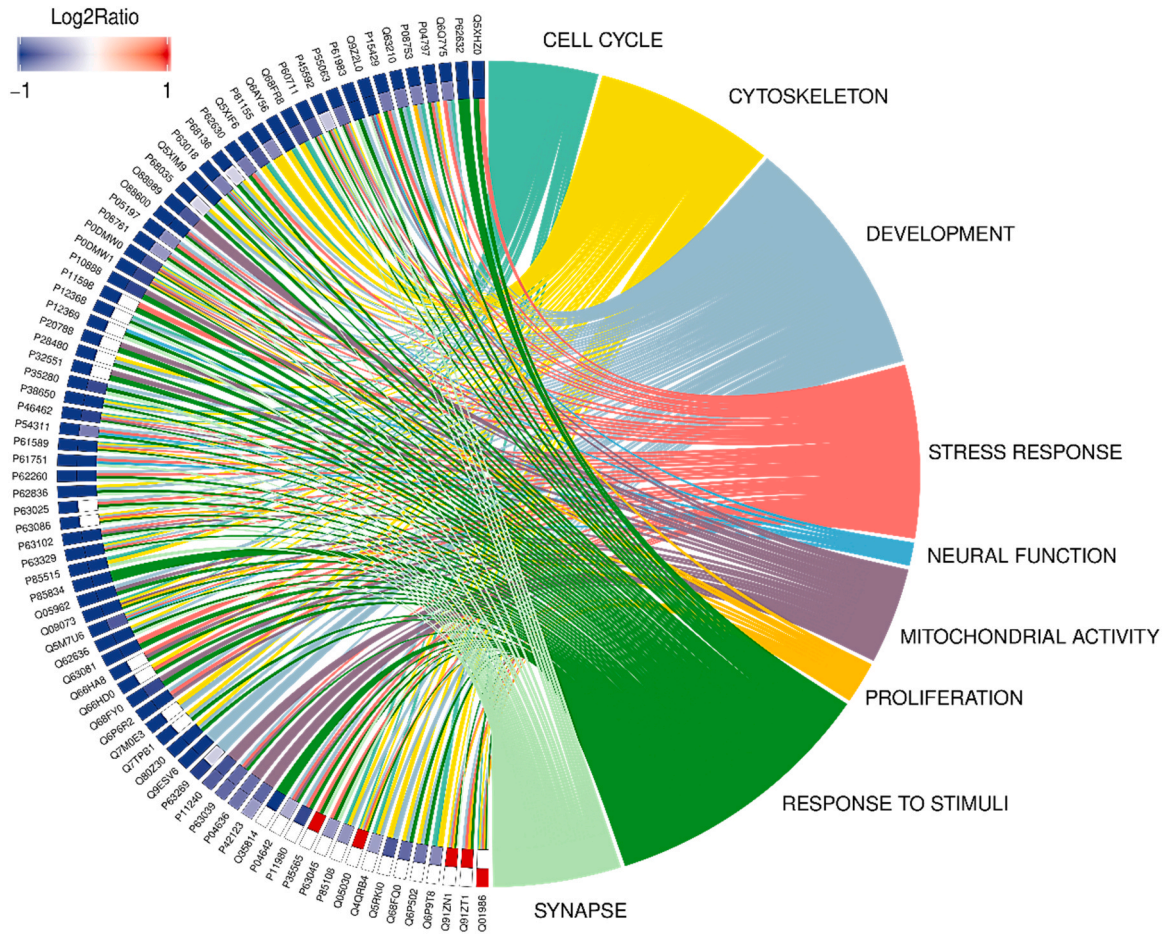

Fig. 7. Circos plot of protein–protein interaction (PPI) in the offspring's hippocampus exposed to 10 mg/L and 50 mg/L of F when compared to the control group in categories cell cycle (turquoise), cytoskeleton (yellow), development (light blue), stress response (pink), neural function (blue), mitochondrial activity (purple), proliferation (gold), response to stimuli (green) and synapse (palegreen). Blue-scale proteins are down-regulated and red up-regulated in the exposed group when compared to the control group. (For interpretation of the references to colour in this figure legend, the reader is referred to the web version of this article.)

and nitrites levels. In comparison to the mature brain, F exposure increases the vulnerability of the developing nervous system to lesions caused by toxic substances, which can become permanent damage (Grandjean and Landrigan, 2006). This mechanism of toxicity consists of a cellular oxidative imbalance with increased levels of prooxidant compounds in comparison to antioxidant compounds (Lu, 2009); thus, several metabolic changes including the oxidation of proteins, enzymes, lipids, DNA and RNA molecules are observed (Schafer et al., 2001). Due to the high oxygen demand of the CNS, ROS levels are physiologically higher than antioxidant defenses and the hippocampus is more susceptible to damage (Hogg and Kalyanaraman, 1999). Considering that the oxidative balance can be modified through enzymatic or non-enzymatic pathways, this study investigated whether the F concentrations could influence any level of the oxidative balance of offspring rats.

Therefore, the influence of F on LPO, antioxidant capacity and nitrite levels in the hippocampal region was evaluated. In comparison to control, the exposed groups showed an increase of MDA levels that indicates LPO. This is a characteristic event of oxidative stress due to the oxidation of cellular lipid membranes, which can even result in cell death (Lu, 2009). Presumably, irreversible damage to the neuronal population was caused by cell death due to oxidative stress at both F concentrations (Schafer et al., 2001). Both F exposed groups presented high nitrite levels, which is an important marker of oxidative stress. Nitrite ions derived from the metabolism of nitric oxide (NO) are indirect markers of oxidative stress (Bains and Hall, 2012; Hogg and Kalyanaraman, 1999).

Some enzymatic antioxidant compounds play a role in the protection and maintenance of cellular redox reactions. These compounds are composed of superoxide dismutase (SOD), catalase (CAT), and glutathione peroxidase (GPx) that neutralize and inhibit the production of ROS and RNS (Ratnam et al., 2006). However, the increase in ROS generation causes oxidative damage that eventually cannot be attenuated by the damaged antioxidant system (He et al., 2017). The excessive ROS generation results in an ineffective antioxidant system with limited influence on cellular redox balance (He et al., 2017). The results of this study revealed a reduction of the ACAP in both F exposed groups as a consequence of oxidative stress that causes physiological changes in several cellular enzymes and biochemical pathways responsible for homeostasis maintenance (Aragão et al., 2018).

In addition, the reduction of antioxidant defenses may lead to changes in hippocampal neurogenesis by increasing ROS (Rola et al., 2007). The hippocampus is known for the constant cellular renewal in the dentate gyrus region, in which neuronal progenitor cells proliferate and differentiate into astrocytes (Kuhn et al., 1996). Oxidative stress also results in the alteration of neuronal structure with impairment of cellular dendritic networks (Huang et al., 2015), which are responsible for maintaining several hippocampal synaptic connections and the functioning of learning-associated memory processes (Stuart and Spruston, 2015). The redox imbalance may change the shape and size of dendritic structures and impair excitatory synapses (Corniola et al., 2012; Fernandez-Fernandez et al., 2018). The association between SOD deficiency and a marked reduction in the thickness and density of granular and pyramidal dendritic cells was reported in an animal study (Zou et al., 2012).

Considering that F can cross the blood–brain barrier (Grandjean and

Landrigan, 2006), the level of this neurotoxic ion also modulates several CNS functions through redox imbalance including the expression of several neurotrophins such as the BDNF in the hippocampal region. This study showed that F exposure at both 10 mg/L and 50 mg/L during pregnancy and lactation increases BDNF expression. As previously mentioned, the redox imbalance is associated with BDNF overexpression since this neurotrophin may induce the phosphorylation of NADPH oxidase and trigger oxidative stress followed by cellular degeneration (Kim et al., 2002). Moreover, BDNF overexpression may be associated with increased synthesis by the endothelial vascular cells of the CNS during oxidative stress (Wang et al., 2006). Several studies reported an increased BDNF expression in the hippocampus as an attempt to neutralize the neurotoxic damage caused by F (Chen et al., 2018; Ma et al., 2015). However, this overexpression may also be associated with proinflammatory conditions featured by BNDF binding to the nuclear factor-kappa B (NF-κB), which in turn is associated with cellular growth functions and the development of inflammatory processes that induce the expression of other pro-apoptotic genes (Mattson et al., 2006).

The redox imbalance caused by F also changed the modulation of heat shock proteins (HSP), which are markers of cellular oxidative stress and proteostasis (Niforou et al., 2014). The proteomic analysis showed that several HSP were down-regulated in both 10 mg/L and 50 mg/L groups, which suggests that the oxidative/nitrosative stress might be a mechanism of damage to the rats' hippocampus and a causal factor for the significant proteome imbalance. In addition to the redox imbalance, peroxiredoxin proteins 2 and 6 (P35704 and O35244, respectively) were found down-regulated in the 50 mg/L group. These proteins are responsible for reducing phospholipid hydroperoxides (Fisher, 2017) and participate in the antioxidant activity (Rhee, 2016).

There is consensus that mitochondria play a key role in energy metabolism and ROS (Hagmann, 2008). In this study, the proteomic analysis showed several cytochrome c (Cytc) subunits exclusively expressed in the control group when compared to the 10 mg/L group (supplementary material) and down-regulation of subunits 1 (P10888), 2 (P00406), and 5A (P11240) in the 50 mg/L group. The Cytc participates in the electron transport chain, apoptosome formation, and apoptosis progression (Hüttemann et al., 2011). Excessive ROS concentration is associated with mitochondrial membrane damages, which may lead to mitochondrial failure and energy impairment (Petrosillo et al., 2013). Thus considering the energy demand of the CNS, any mitochondrial impairment could result in functional deficits (Beal, 2005; Boveris and Navarro, 2008).

This research group recently showed that F impairs liver mitochondria function on a time and dose-dependent manner (Araujo et al., 2019) and the present proteomic analysis also indicated some effects of F exposure during pregnancy and lactation of offspring rats on energy metabolism-related proteins: down-regulation of ATP synthase subunits in both 10 mg/L (P15999, P10719) and 50 mg/L groups (P15999, P10719, P31399, Q06647); exclusive expression in the control group when compared to the 10 mg/L group (P19511, P31399, P35435, Q06647, P21571); proteins related to the metabolism of other molecules such as aspartate aminotransferase (P13221 and P00507, down-regulated in the 10 mg/L group), isocitrate dehydrogenase subunits (Q99NA5, P41565, only expressed in the control group in comparison to the 10 mg F/L group), Acetyl CoA acetyltransferase (P17764) and citrate synthase (Q8VHF5, down-regulated in the 50 mg/L group).

Failures in mitochondrial function are associated with the aging process and neurodegenerative diseases (Beal, 2005). This experimental model with offspring rats raises an important question since F triggered several oxidative/nitrosative and energetic imbalances that create an improper microenvironment for a developing CNS. Thus, the proteome of rats exposed to 10 mg/L and 50 mg/L showed deregulation of several synapse-related proteins. The lowest F concentration down-regulated the clathrin heavy chain 1 (P11442), Synapsin 1 (P09951) and 2 (Q63537), Synaptophysin (P07825) and Vesicle-fusing ATPase (Q9QUL6). The highest F concentration also down-regulated the Clathrin coat assembly protein AP180 (Q05140, Q63537 and P07825) and the Excitatory amino acid transporter 2 (P31596).

The protein S100β (P04631) is mainly involved in glial and neural progenitor differentiation and expansion in the early stages (Sorci et al., 2013). Although its pathway in astrocyte differentiation is not fully elucidated, some evidence indicates that the stimulation of RhoA/ROCK by Src/PI3K results in proliferation and inhibition of differentiation (Brozzi et al., 2009). Interestingly, this proteomic analysis revealed a down-regulation of S100β in the 50 mg/L group and an exclusive expression in the 10 mg/L group. Also, the SRC kinase signaling inhibitor 1 (Q9QXY2) was expressed only in the control group in comparison to the 50 mg/L group, which suggests an imbalance in this pathway. The Glial fibrillary acidic protein (P47819), which is essential for astrocyte development and reactivity (Wilhelmsson et al., 2019), was found down-regulated in the 50 mg/L group and thus the null hypotheses that the higher F concentration does not lead to CNS impairments can be rejected.

The various results found in the proteomic profile were objectively categorized in accordance with their function in the over-representation analysis (ORA); thus, the down-regulated protein groups can be observed in the 10 mg/L and 50 mg/L groups. The proteins associated with oxidative stress (P11598), which participated in the redox homeostasis (Laurindo et al., 2012), were absent in the 50 mg/L group and downregulated in the 10 mg/L group. Modulations of the cytochrome oxidase proteins (P11240 and P32551) that control the generation of free radicals in the mitochondria (Yu et al., 2018) and the HSP (Q66HD0 and Q7TPB1) involved in the process, transport, and folding of cellular proteins were observed (Bromfield and Nixon, 2013; Kubota et al., 1995). Changes in these protein groups may modulate multiple functions (protein folding, unfolding, and remodeling) related to the protection and stability of the proteome (Bukau et al., 2006).

The attempt to attenuate this degradation process was represented by the over-representation of the Calnexin protein (P35565) that maintains the quality of the proteins synthesized in the endoplasmic reticulum and retains incorrectly folded proteins. The PDGF-B protein (Q05030), which is linked to neuroprotection through detoxification of free radicals, was also found (Zheng et al., 2010). *In vitro* and in vivo studies indicated that PDGF-B has a neuroprotective effect against the oxidative stress generated by hydrogen peroxide (H_2O_2), prevents the neuronal death with the main pathways involved in the phosphoinositide-3-kinase (PI3-K/Akt) and the microtubule-associated proteins (MAPs) (Iihara et al., 1997; Pietz et al., 1996; Zheng et al., 2010). The cAMP-dependent protein kinase type II-beta was also absent in the 50 mg/L group. This protein participates in synaptic communication through the activation of protein kinases (P12369) and is also associated with long-term potentiation (LTP); thus, molecular changes associated with learning can be found in this F exposure period.

In this context, the vesicle-associated membrane protein 3 (P63025) that forms the SNARE complex (soluble NSF attachment receptor) was absent in the group with the highest F concentration (50 mg/L). This protein couples the synaptic vesicle membrane and participates in the regulation of the vesicular transport and the exocytosis in the presynaptic terminal to release neurotransmitters. The reduced activity of this protein changes the vesicular transport, impairs reactions in the synaptic cleft, decreases the release of neurotransmitters, and compromises the hippocampal functionality (Sinha et al., 2011). Therefore, one can suggest that high F concentrations (as in the 50 mg/L group) induced functional alterations in hippocampal neural cells that contributed to the reduction of synaptic transmissions and consequent cognitive dysfunction (Jiang et al., 2014b; Niu et al., 2009).

5. Conclusion

The exposure to F in the pregnancy and lactation period was able to promote oxidative biochemical imbalance in the offsprings' hippocampus, which in turn increased the level of expression of BDNF and

modulated the proteomic profile in the hippocampal region. Our study was able to show that exposure to F during pregnancy and lactation can already trigger several changes in the hippocampus of the offspring. Our results direct new questions regarding the possible repercussions on the hippocampal structure and its functioning in the different types of memories executed by this brain region.

Data availability

The data used to support the findings of this study are available from the corresponding author upon request.

Funding statement

This work was supported by Pró-Reitoria de Pesquisa da UFPA (PROPESP, UFPA, Brazil), Brazilian National Council for Scientific and Technological Development (CNPq, Grant n. 435093/2018-5) and Coordenação de Aperfeiçoamento de Pessoal de Nível Superior (CAPES)-Finance Code 001.

CRediT authorship contribution statement

Ferreira MKM: Investigation, Data curation, Writing - original draft. **Aragão WAB:** Investigation, Data curation, Writing - Original draft. **Bittencourt LO:** Investigation, Data curation, Writing - Original draft. **Puty BG:** Investigation, Software, Writing - review & editing. **Dionizio A:** Investigation, Software, Writing - review & editing. **de Souza MPC:** Investigation, Software. **Buzalaf MAR:** Investigation, Software, Writing - review & editing, Resources, Formal analysis. **de Oliveira EH:** Investigation, Software, Writing - review & editing; resources. **Lopez MEC:** Investigation, Writing - review & editing; data curation. **Lima RR:** Investigation, Writing - review & editing, Conceptualization, Supervision, Resources.

Declaration of Competing Interest

The authors declare that they have no known competing financial interests or personal relationships that could have appeared to influence the work reported in this paper.

Appendix A. Supporting information

Supplementary data associated with this article can be found in the online version at doi:10.1016/j.ecoenv.2020.111437.

References

Alhamdoosh, M., et al., 2017. Combining multiple tools outperforms individual methods in gene set enrichment analyses. Bioinformatics 33, 414–424.
Amado, L.L., et al., 2009. A method to measure total antioxidant capacity against peroxyl radicals in aquatic organisms: application to evaluate microcystins toxicity. Sci Total Environ. 407, 2115–2123.
Aragão, W.A.B., Teixeira, F.B., Fagundes, N.C.F., Fernandes, R.M., Fernandes, L.M.P., da Silva, M.C.F., Amado, L.L., Sagica, F.E.S., Oliveira, E.H.C., Crespo-Lopez, M.E., Maia, C.S.F., Lima, R.R., 2018. Hippocampal dysfunction provoked by mercury chloride exposure: evaluation of cognitive impairment, oxidative stress, tissue injury and nature of cell death. Oxid. Med. Cell. Longev. 2018, 1–11.
Araujo, T.T., et al., 2019. Changes in energy metabolism induced by fluoride: insights from inside the mitochondria. Chemosphere 236, 124357.
Bains, M., Hall, E.D., 2012. Antioxidant therapies in traumatic brain and spinal cord injury. Biochim Biophys Acta. 1822, 675–684.
Barker, G.R., Warburton, E.C., 2015. Object-in-place associative recognition memory depends on glutamate receptor neurotransmission within two defined hippocampal-cortical circuits: a critical role for AMPA and NMDA receptors in the hippocampus, perirhinal, and prefrontal cortices. Cereb. Cortex 25, 472–481.
Bashash, M., et al., 2018. Prenatal fluoride exposure and attention deficit hyperactivity disorder (ADHD) symptoms in children at 6–12 years of age in Mexico City. Environ Int. 121, 658–666.
Beal, M.F., 2005. Mitochondria take center stage in aging and neurodegeneration. Ann. Neurol. 58, 495–505.
Bindea, G., et al., 2009. ClueGO: a Cytoscape plug-in to decipher functionally grouped gene ontology and pathway annotation networks. Bioinformatics 25, 1091–1093.
Bittencourt, L.O., Dionizio, A., Nascimento, P.C., Puty, B., Leão, L.K.R., Luz, D.A., Silva, M.C.F., Amado, L.L., Leite, A., Buzalaf, M.R., Crespo-Lopez, M.E., Maia, C.S.F., Lima, R.R., 2019. Proteomic approach underlying the hippocampal neurodegeneration caused by low doses of methylmercury after long-term exposure in adult rats. Metallomics 11, 390–403.
Boveris, A., Navarro, A., 2008. Brain mitochondrial dysfunction in aging. IUBMB Life 60, 308–314.
Bradford, M.M., 1976. A rapid and sensitive method for the quantitation of microgram quantities of protein utilizing the principle of protein-dye binding. Anal. Biochem. 72, 248–254.
Broadbent, N.J., Squire, L.R., Clark, R.E., 2004. Spatial memory, recognition memory, and the hippocampus. Proc. Natl. Acad. Sci. USA 101, 14515–14520.
Bromfield, E.G., Nixon, B.J.R., 2013. The function of chaperone proteins in the assemblage of protein complexes involved in gamete adhesion and fusion processes. Reproduction 145, R31–R42.
Brozzi, F., 2009. S100B Protein regulates astrocyte shape and migration via interaction with Src kinase implications for astrocyte development, activation, and tumor growth. J. Biol. Chem. 284, 8797–8811.
Bukau, B., 2006. Molecular chaperones and protein quality control. Cell. 125, 443–451.
Bustin, S.A., et al., 2009. The MIQE Guidelines: Minimum Information for Publication of Quantitative Real-Time PCR Experiments. Oxford University Press.
Buzalaf, M.A.R., Pessan, J.P., Honório, H.M., Ten Cate, J.M., 2011. Mechanisms of action of fluoride for caries control. Monogr. Oral. Sci. 22, 97–114. https://doi.org/10.1159/000325151.
Chen, J., Niu, Q., Xia, T., Zhou, G., Li, P., Zhao, Q., Xu, C., Dong, L., Zhang, S., Wang, A., 2018. ERK1/2-mediated disruption of BDNF-TrkB signaling causes synaptic impairment contributing to fluoride-induced developmental neurotoxicity. Toxicology 410, 222–230.
Clark, R.E., Zola, S.M., Squire, L.R., 2000. Impaired recognition memory in rats after damage to the hippocampus. J. Neurosci. 20, 8853–8860.
Corniola, R., et al., 2012. Paradoxical relationship between Mn superoxide dismutase deficiency and radiation-induced cognitive defects. PLoS One 7, e49367.
Corrêa, M.G., Bittencourt, L.O., Nascimento, P.C., Ferreira, R.O., Aragão, W.A.B., Silva, M.C.F., Gomes-Leal, W., Fernandes, M.S., Dionizio, A., Buzalaf, M.R., Crespo-Lopez, M.E., Lima, R.R., 2020. Spinal cord neurodegeneration after inorganic mercury long-term exposure in adult rats: ultrastructural, proteomic and biochemical damages associated with reduced neuronal density. Ecotoxicol. Environ. Saf. 191, 110159.
Cury, J.A., et al., 2019. Systemic effects (risks) of water fluoridation. Brazilian Dental J. 30, 421–428.
Dec, K., Łukomska, A., Maciejewska, D., Jakubczyk, K., Baranowska-Bosiacka, I., Chlubek, D., Wąsik, A., Gutowska, I., 2017. The influence of fluorine on the disturbances of homeostasis in the central nervous system. Biol. Trace Elem. Res. 177, 224–234.
Dec, K., Łukomska, A., Skonieczna-Żydecka, K., Kolasa-Wołosiuk, A., Tarnowski, M., Baranowska-Bosiacka, I., Gutowska, I., 2019. Long-term exposure to fluoride as a factor promoting changes in the expression and activity of cyclooxygenases (COX1 and COX2) in various rat brain structures. Neurotoxicology 74, 81–90.
Dhar, V., Bhatnagar, M., 2009. Physiology and toxicity of fluoride. Indian J. Dent Res. 20, 350.
Dionizio, A.S., et al., 2018. Chronic treatment with fluoride affects the jejunum: insights from proteomics and enteric innervation analysis. Sci. Rep. 8, 1–12.
Dunipace, A.J., Brizendine, E.J., Zhang, W., Wilson, M.E., Miller, L.L., Katz, B.P., Warrick, J.M., Stookey, G.K., 1995. Effect of aging on animal response to chronic fluoride exposure. J. Dent. Res. 74, 358–368.
Esterbauer, H., Cheeseman, K.H., 1990. Determination of aldehydic lipid peroxidation products: malonaldehyde and 4-hydroxynonenal. Methods Enzymol. 186, 407–421. https://doi.org/10.1016/0076-6879(90)86134-h.
Fernandez-Fernandez, S., et al., 2018. Hippocampal neurons require a large pool of glutathione to sustain dendrite integrity and cognitive function. Redox Biol. 19, 52–61.
Fisher, A.B., 2017. Peroxiredoxin 6 in the repair of peroxidized cell membranes and cell signaling. Arch. Biochem. Biophys. 617, 68–83.
Grandjean, P., Landrigan, P., 2006. Developmental neurotoxicity of industrial chemicals. Lancet. 368, 2167–2178.
Green, L.C., Wagner, D.A., Glogowski, J., Skipper, P.L., Wishnok, J.S., Tannenbaum, S.R., 1982. Analysis of nitrate, nitrite, and [15N]nitrate in biological fluids. Anal. Biochem. 126 (1), 131–138. https://doi.org/10.1016/0003-2697(82)90118-x.
Hagmann, W.K., 2008. The many roles for fluorine in medicinal chemistry. J. Med. Chem. 51, 4359–4369.
He, L., et al., 2017. Antioxidants maintain cellular redox homeostasis by elimination of reactive oxygen species. Cell. Physiol. Biochem. 44, 532–553.
Hogg, N., Kalyanaraman, B., 1999. Nitric oxide and lipid peroxidation. Biochim. Biophys. Acta 1411, 378–384.
Huang, T.-T., et al., 2015. Oxidative stress and redox regulation on hippocampal-dependent cognitive functions. Arch. Biochem. Biophys. 576, 2–7.
Hüttemann, M., Pecina, P., Rainbolt, M., Sanderson, T.H., Kagan, V.E., Samavati, L., Doan, J.W., Lee, I., 2011. The multiple functions of cytochrome c and their regulation in life and death decisions of the mammalian cell: from respiration to apoptosis. Mitochondrion 11, 369–381.
Iihara, K., et al., 1997. Platelet-derived growth factor-BB, but not-AA, prevents delayed neuronal death after forebrain ischemia in rats. J. Cereb. Blood. Flow. Metab. 17, 1097–1106.
Jiang, C., et al., 2014a. Low glucose utilization and neurodegenerative changes caused by sodium fluoride exposure in rat's developmental brain. Neuromolecular Med. 16, 94–105.

Jiang, S., Su, J., Yao, S., Zhang, Y., Cao, F., Wang, F., Wang, H., Li, J., Xi, S., 2014b. Fluoride and arsenic exposure impairs learning and memory and decreases mGluR5 expression in the hippocampus and cortex in rats. PLoS One 9, e96041.
Karimzade, S., et al., 2014. Investigation of intelligence quotient in 9–12-year-old children exposed to high-and low-drinking water fluoride in West Azerbaijan Province. Iran 47, 9–14.
Katz, S., Stookey, G.K., 1973. Further studies concerning the placental transfer of fluoride in the rat. J. Dent. Res. 52, 206–210.
Kim, S.H., Won, S.J., Sohn, S., Kwon, H.J., Lee, J.Y., Park, J.H., Gwag, B.J., 2002. Brain-derived neurotrophic factor can act as a pronecrotic factor through transcriptional and translational activation of NADPH oxidase. J. Cell Biol. 159, 821–831.
Kinawy, A.A., Research, P., 2019. Synergistic oxidative impact of aluminum chloride and sodium fluoride exposure during early stages of brain development in the rat. Environ. Sci. Pollut. Res. Int. 26, 10951–10960.
Kubota, H., 1995. The chaperonin containing t-complex polypeptide 1 (TCP-1) multisubunit machinery assisting in protein folding and assembly in the eukaryotic cytosol. Eur. J. Biochem. 230, 3–16.
Kuhn, H.G., et al., 1996. Neurogenesis in the dentate gyrus of the adult rat: age-related decrease of neuronal progenitor proliferation. J. Neurosci. 16, 2027–2033.
Laurindo, F.R.M., Pescatore, L.A., de Castro Fernandes, D., 2012. Protein disulfide isomerase in redox cell signaling and homeostasis. Free Radic. Biol. Med. 52, 1954–1969.
Li, X., Zhang, J., Niu, R., Manthari, R.K., Yang, K., Wang, J., 2019. Effect of fluoride exposure on anxiety- and depression-like behavior in mouse. Chemosphere 215, 454–460.
Lima Leite, A., et al., 2014. Proteomic analysis of gastrocnemius muscle in rats with streptozotocin-induced diabetes and chronically exposed to fluoride. PLoS One 9 e106646-e106646.
Liu, F., Ma, J., Zhang, H., Liu, P., Liu, Y.P., Xing, B., Dang, Y.H., 2014. Fluoride exposure during development affects both cognition and emotion in mice. Physiol. Behav. 124, 1–7.
Livak, K.J., Schmittgen, T.D., 2001. Analysis of relative gene expression data using real-time quantitative PCR and the 2− ΔΔCT method. Methods 25, 402–408.
Lu, J., 2009. Systemic inflammatory response following acute traumatic brain injury. Front. Biosci. (Landmark Ed.) 14, 3795–3813.
Ma, J., et al., 2015. Impact of early developmental fluoride exposure on the peripheral pain sensitivity in mice. Int. J. Dev. Neurosci. 47, 165–171.
Mattson, M., et al., 2006. Roles for NF-κB in nerve cell survival, plasticity, and disease. Cell. Death Differ. 13, 852.
Miranda, G.H.N., Gomes, B.A.Q., Bittencourt, L.O., Aragão, W.A.B., Nogueira, L.S., Dionizio, A.S., Buzalaf, M.A.R., Monteiro, M.C., Lima, R.R., 2018. Chronic exposure to sodium fluoride triggers oxidative biochemistry misbalance in mice: effects on peripheral blood circulation. Oxid. Med. Cell. Longev. 2018, 8379123-8379123.
Niforou, K., Cheimonidou, C., Trougakos, I.P., 2014. Molecular chaperones and proteostasis regulation during redox imbalance. Redox Biol. 2, 323–332.
Niu, R., Chen, H., Manthari, R.K., Sun, Z., Wang, J., Zhang, J., Wang, J., 2018. Effects of fluoride on synapse morphology and myelin damage in mouse hippocampus. Chemosphere 194, 628–633.
Niu, R., et al., 2009. Decreased learning ability and low hippocampus glutamate in offspring rats exposed to fluoride and lead. Environ. Toxic. Pharm. 28, 254–258.
Ozsvath, D.L., Bio/Technology, 2009. Fluoride and environmental health: a review. Rev. Environ. Sci. Biotechnol. 8, 59–79.
Petrosillo, G., et al., 2013. Decline in cytochrome C oxidase activity in rat-brain mitochondria with aging. Role of peroxidized cardiolipin and beneficial effect of melatonin. J. Bioenerg. Biomembr. 45, 431–440.
Pietz, K., et al., 1996. Protective effect of platelet-derived growth factor against 6-hydroxydopamine-induced lesion of rat dopaminergic neurons in culture. Neurosci Lett. 204, 101–104.
Qian, W., et al., 2013. Effect of selenium on fluoride-induced changes in synaptic plasticity in rat hippocampus. Biol. Trace Elem. Res. 155, 253–260.
Ratnam, D.V., et al., 2006. Role of antioxidants in prophylaxis and therapy: a pharmaceutical perspective. J. Control Release 113, 189–207.
Rhee, S.G., 2016. Overview on peroxiredoxin. Mol. Cells 39, 1–5.
Rola, R., et al., 2007. Lack of extracellular superoxide dismutase (EC-SOD) in the microenvironment impacts radiation-induced changes in neurogenesis. Free Radic. Biol. Med. 42, 1133–1145.
Saxena, S., Sahay, A., Goel, P., 2012. Effect of fluoride exposure on the intelligence of school children in Madhya Pradesh, India. J. Neurosci. Rural Pract. 3, 144–149.
Schafer, F.Q., et al., 2001. Redox environment of the cell as viewed through the redox state of the glutathione disulfide/glutathione couple. Free Radic Biol. Med. 30, 1191–1212.
Shannon, P., et al., 2003. Cytoscape: a software environment for integrated models of biomolecular interaction networks. Genome Res. 13, 2498–2504.
Shenoy, P.S., et al., 2019. Sodium fluoride induced skeletal muscle changes: degradation of proteins and signaling mechanism. In: Environ. Pollut. (Barking, Essex : 1987), pp. 534–548.
Shivaprakash, P., Noorani, H., Ohri, K., 2011. Relation between dental fluorosis and intelligence quotient in school children of Bagalkot district. J. Indian Soc. Pedod. Prev. Dent. 29, 117–120.
Shivarajashankara, Y., et al., 2002. Brain lipid peroxidation and antioxidant systems of young rats in chronic fluoride intoxication. Fluoride 35, 197–203.
Sinha, R., Ahmed, S., Jahn, R., Klingauf, J., 2011. Two synaptobrevin molecules are sufficient for vesicle fusion in central nervous system synapses. Proc. Natl. Acad. Sci. USA 108, 14318–14323.
Sorci, G., et al., 2013. S100B protein in tissue development, repair and regeneration. World J. Biol. Chem. 4, 1.
Squire, L.R., 1992. Memory and the hippocampus: a synthesis from findings with rats, monkeys, and humans. Psychol. Rev. 99, 195–231.
Stuart, G.J., Spruston, N., 2015. Dendritic integration: 60 years of progress. Nat. Neurosci 18, 1713.
Tang, Q.-Q., et al., 2008. Fluoride and children's intelligence: a meta-analysis. Biol. Trace Elem. Res. 126, 115–120.
Taves, D.R.J.T., 1968. Separation of fluoride by rapid diffusion using hexamethyldisiloxane. Talanta 15, 969–974.
Team, R.C., 2013. R: a language and environment for statistical computing.
Toyama, Y., Nakagaki, H., Kato, S., Huang, S., Mizutani, Y., Kojima, S., Toyama, A., Ohno, N., Tsuchiya, T., Kirkham, J., Robinson, C., 2001. Fluoride concentrations at and near the neonatal line in human deciduous tooth enamel obtained from a naturally fluoridated and a non-fluoridated area. Arch. Oral Biol. 46, 147–153.
Trivedi, M., et al., 2012. Assessment of groundwater quality with special reference to fluoride and its impact on IQ of schoolchildren in six villages of the Mundra region, Kachchh, Gujarat, India. Fluoride 45, 377–383.
Varner, J.A., et al., 1998. Chronic administration of aluminum–fluoride or sodium–fluoride to rats in drinking water: alterations in neuronal and cerebrovascular integrity. Brain Res. 784, 284–298.
Wang, H., Ward, N., Boswell, M., Katz, D.M., 2006. Secretion of brain-derived neurotrophic factor from brain microvascular endothelial cells. Eur. J. Neurosci. 23, 1665–1670.
Whitford, G.M., 2011. Acute toxicity of ingested fluoride. Monogr. Oral Sci. 22, 66–80.
Wilhelmsson, U., et al., 2019. The role of GFAP and vimentin in learning and memory. Biol. Chem. 400, 1147–1156.
Xia, J., et al., 2014. NetworkAnalyst-integrative approaches for protein–protein interaction network analysis and visual exploration. Nucleic Acids Res. 42, W167–W174.
Yu, H., Wang, D., Zou, L., Zhang, Z., Xu, H., Zhu, F., Ren, X., Xu, B., Yuan, J., Liu, J., Spencer, P.S., Yang, X., 2018. Proteomic alterations of brain subcellular organelles caused by low-dose copper exposure: implication for Alzheimer's disease. Arch. Toxicol. 92, 1363–1382.
Zhang, Z., et al., 1999. Effect of fluoride exposure on synaptic structure of brain areas related to learning-memory in mice. Chinese 28, 210.
Zheng, L., et al., 2010. Neuroprotective effects of PDGF against oxidative stress and the signaling pathway involved. J. Neurosci. Res. 88, 1273–1284.
Zhu, Y., Xi, S., Li, M., Ding, T., Liu, N., Cao, F., Zeng, Y., Liu, X., Tong, J., Jiang, S., 2017. Fluoride and arsenic exposure affects spatial memory and activates the ERK/CREB signaling pathway in offspring rats. Neurotoxicology 59, 56–64.
Zou, Y., et al., 2012. Extracellular superoxide dismutase is important for hippocampal neurogenesis and preservation of cognitive functions after irradiation. Proc. Natl. Acad Sci. 109, 21522–21527.